Influence of Persulfate on Transformation of Phosphorus and Heavy Metals for Improving Sewage Sludge Dewaterability by Hydrothermal Treatment

Qiao Xiong
Huazhong University of Science and Technology
Jing Xia
Design and Research Institute, Wuhan University of Technology
Xiang Wu
Huazhong University of Science and Technology
Xu Wu
Huazhong University of Science and Technology
Haobo Hou
Wuhan University
Hang Lv (lvhang@hust.edu.cn)
Huazhong University of Science and Technology

Research Article

Keywords: Persulfate, Hydrothermal treatment, Sludge dewaterability, Phosphorus, Heavy metals, Box-Behnken design

Posted Date: June 23rd, 2021

DOI: https://doi.org/10.21203/rs.3.rs-431772/v1

Version of Record: A version of this preprint was published at Environmental Science and Pollution Research on January 13th, 2022. See the published version at https://doi.org/10.1007/s11356-022-18624-1.

Influence of persulfate on transformation of phosphorus and heavy metals for improving sewage sludge dewaterability by hydrothermal treatment

Qiao Xiong[a], Jing Xia[b], Xiang Wu[a], Xu Wu[a], Haobo Hou[c], Hang Lv[a*]

a. School of Environmental Science and Engineering, Huazhong University of Science and Technology, Wuhan 430074, China

b. Design and Research Institute, Wuhan University of Technology, Wuhan 430070, China

c. School of Resource and Environment Science, Wuhan University, Wuhan 430072, China

Abstract

Activated persulfate oxidation has been proven to be an efficient advanced sludge treatment technique to improve sludge dewaterability. This study investigates the influence of persulfate on the transformation of phosphorus (P) and heavy metals (HMs) during the hydrothermal treatment of sewage sludge. The hydrothermal temperature, time, and persulfate concentration are optimized by a Box-Behnken design to obtain the best sludge dewaterability, which is expressed by capillary suction time (CST). The highest CST reduction efficiency is 90.5% at the optimal hydrothermal temperature, time and concentration of persulfate, which are 145 °C, 2 h, and 150 mg/g DS, respectively. The distribution and transformation of P and HMs with different persulfate concentrations (100-200 mg/g DS) during the hydrothermal process are investigated. Results show that more than 90% of the P and HMs in the sludge are retained in sludge cakes after the hydrothermal treatment. The addition of SPS can make the P in the sludge cakes transform into more stable P species according to the extraction capacity of sequential extracts. It can be found from the ecological risk indexes of the HMs that the addition of SPS during the hydrothermal treatment of sludge can reduce the environmental risk of HMs. This study provides insights into the P and HM distribution and transformation during hydrothermal treatment with persulfate, providing a reference for sludge recovery strategies.

Keywords: Persulfate, Hydrothermal treatment, Sludge dewaterability, Phosphorus, Heavy metals, Box-Behnken design

1. Introduction

With the wide application of biological sewage treatment technology, a considerable quantity of sewage sludge is produced as a by-product during wastewater treatment (Neyens et al., 2004). Sewage sludge is a useful waste containing valuable resources, such as organic carbon, phosphorous (P) and nitrogen (N), along with hazardous substances, such as pathogens, heavy metals (HMs) and persistent organic pollutants (Zhang et al., 2009, Świerczek et al., 2018, Mahmoud et al., 2018). Therefore, sludge requires reasonable treatment and disposal before entering the environment. To reduce the costs of sludge transportation and disposal, a reduction of the sludge volume by solid-water separation is an essential step prior to sludge disposal (Li et al., 2018). Many technologies have been explored to improve sludge dewaterability, which is a key point for sludge volume reduction, including electro-dewatering technology (Saveyn et al., 2005), chemical conditioning (Xu et al., 2018), and thermal drying (Olivier et al., 2015). Notably, hydrothermal treatment has proven to be an effective pretreatment method to enhance sludge dewaterability owing to the solubilization of organic matter (Kepp et al., 2000). Additionally, hydrothermal treatment can reduce sludge toxicity, control HMs, and recover resources (e.g., P and N) and energy from biosolids (Dewil et al., 2007; Funke and Ziegler, 2010).

On the other hand, the persulfate advanced oxidation process has been widely used to improve sludge dewaterability due to its high solubility, strong oxidation potential, and resistance to pH changes (Zhen et al., 2012). Persulfate can be activated by heat to produce sulfate radicals with strong oxidizability (Kordkandi and Forouzesh, 2014).

Therefore, combing a hydrothermal treatment with persulfate can not only can intrinsically enhance sludge dewaterability but also activate persulfate to generate sulfate radicals, which can further improve sludge dewatering.

The effects of hydrothermal treatment conditions on nutrient element (i.e., P and N) transformation, solid product properties, and HM risk have been widely investigated. Yu et al. (2019) investigated the effect of metal ions on P speciation during hydrothermal treatment, and their results showed that P immobilization was significantly influenced by the metal contents. Huang and Yuan (2016) studied the effects of temperature, time, and the addition of catalyst on the fate of HMs during the hydrothermal treatment of sewage sludge. It was concluded that the total concentration of HMs in solid products increased with an increasing temperature, and a proper catalyst addition could enhance the immobilization of HMs in the solid products. Zhang et al. (2017) speculated on the pathway of N transformation during the hydrothermal treatment of sewage sludge, and the results indicated that only 20% N remained in the solid product. Even so, little attention has been given to the influence of persulfate on the transformation of P and HMs during the hydrothermal treatment process to enhance sewage sludge dewaterability.

Therefore, different concentrations of persulfate were used to evaluate the bioavailability of P and HMs in sludge cakes produced from hydrothermal treatment. The objectives of this study were (1) to optimize the hydrothermal temperature, time, and concentration of persulfate to achieve the best sludge dewaterability; (2) to evaluate the P transformation and speciation by sequential extracts during the hydrothermal

process; and (3) to investigate the fraction distribution and ecological risk of HMs in the sludge cakes after hydrothermal treatment. Finally, this study sheds light on the transformation of P and HMs during persulfate hydrothermal treatment to enhance sludge dewaterability, providing basic knowledge for sludge reuse.

2. Materials and methods

2.1. Materials

Raw sewage sludge was collected from Zhuankou Wastewater Treatment (Hanyang District, Wuhan, China), air-dried in an oven at 105 °C until it was completely dehydrated, and then ground to powder and passed through a 0.154 mm sieve. The dried sludge powder (RS) was stored in airtight bags for subsequent experiments. This pretreatment avoided biochemical reactions during sludge storage and precisely controlled the mass ratio of sludge to deionized water in the hydrothermal conditioning procedure. The initial characteristics of the raw sewage sludge are provided in Table 1.

Table 1. Main characteristics of the raw sewage sludge.

Parameter	Moisture (%)	pH	Organic content (%)	CST (s)
Value	79.5±1.12	7.1±0.1	48.1±0.65	155±1.05

Sodium persulfate (SPS) ($Na_2S_2O_8$, > 99.9 wt%) (Sinopharm Chemical Reagent, China) was analytical reagent grade and directly used. Deionized water was used as the experimental water.

2.2. Hydrothermal conditioning procedure

Hydrothermal conditioning experiments were performed in a well-designed 500

ml stainless steel reactor that could operate at high temperatures and pressures. RS and deionized water were mixed at a solid content of 10 wt%, then SPS was added and the mixture was stirred at 600 rpm for 60 min before heating. The reactor was heated to the desired temperature and maintained at the final temperature for a certain time. The mixed solution was magnetically stirred at a speed of 150 rpm during the whole hydrothermal conditioning procedure. After conditioning, the reactor was naturally cooled to room temperature, and the suspension was separated by centrifugation at 4000 rpm for 20 min. The solid product was dried at 105 °C for 24 h for further analysis. The liquid product called process water, was filtered through a 0.45 μm filter and stored at 4 °C for subsequent analysis.

To investigate the influence of persulfate on the transformation of P and HMs during the hydrothermal conditioning of sewage sludge, six experiments with different SPS concentrations were conducted, these experiments are shown in Table 2. The sludge samples conditioned with 100 mg/g DS SPS, 125 mg/g DS SPS, 150 mg/g DS SPS, 175 mg/g DS SPS, and 200 mg/g DS SPS at 145 °C are labeled S1, S2, S3, S4, and S5, respectively; the collected sludge cakes were denoted as CS1, CS2, CS3, CS4, and CS5, respectively. The liquid samples are denoted as LS1, LS2, LS3, LS4, and LS5, respectively. Sludge conditioned without the addition of SPS at 145 °C was used as the control and denoted as S0; its relevant liquid samples and sludge cakes were denoted as LS0 and CS0, respectively. In addition, 2 h was selected as the conditioning time according to response surface methodology (RSM) optimization.

Table 2 Different sludge conditioning procedures.

Symbol	pH	Temperature (°C)	Time (h)	SPS concentration (mg/g DS)
S0	7.2±0.2	145	2	0
S1	7.2±0.2	145	2	100
S2	7.2±0.2	145	2	125
S3	7.2±0.2	145	2	150
S4	7.2±0.2	145	2	175
S5	7.2±0.2	145	2	200

2.3. Optimization design

The hydrothermal conditioning time, temperature, and SPS concentration were optimized by using a Box-Behnken design. The ranges and levels of the three constituents shown in Table S1 were determined by a set of preliminary experiments. The CST reduction efficiency was set as the response. Table S2 shows the details of the BBD experimental design and results.

2.4. Quantification of the P and heavy metal content

A combustion method was used to measure the total P content in all solid samples. Specifically, the RS and solid products were first combusted at 600 °C for 2 h in a furnace and then extracted by HCl solution (1 M) for 16 h. Then, the total P in the extract was measured as orthophosphate using the ascorbic acid assay on a UV-vis spectrophotometer (UV-1800).

The total HMs content of all samples was measured using microwave-assisted acid digestion and determined by inductively coupled plasma optical emission spectrometry

(ICP-OES, Perking, Elmer8300, USA).

2.5. Fractionation procedure of the P and HMs

Hedley sequential fractionation was employed to quantify the major speciation of P (Hedley et al., 1982). Briefly, 0.2 g of solid product was placed into a 50 ml centrifuge tube and extracted sequentially with 20 ml of H_2O, $NaHCO_3$ (0.5 M), NaOH (0.1 M), and HCl (1 M) at 25 °C for 16 h. The suspension was centrifuged, and the supernatant was filtered through a 0.45 μm filter and stored at 4 °C for further analysis. The solid residue was used for the next extraction step. The H_2O and $NaHCO_3$ extractable P species (H_2O-P, $NaHCO_3$-P) were ascribed to the readily soluble phosphates and organophosphates. NaOH extractable P species (NaOH-P) were attributed to P sorbed on the Fe/Al mineral phases. HCl extractable P species (HCl-P) were attributed to insoluble phosphate minerals, such as Ca, Al, and Fe phosphates. Finally, P retained in the sample is denoted as Residue-P. The P content in all extracts was analyzed by using an ascorbic acid assay with UV-vis spectrophotometry (UV-1800).

The Community Bureau of Reference (BCR) sequential extraction procedure was conducted to investigate the chemical speciation of HMs (Rauret et al., 1999). The four fractions of metal speciation, included HMs that were soluble and exchangeable (F1), HMs that bound to iron and manganese oxides (reducible) (F2), HMs that bound to organic matter and sulfide (oxidizable) (F3) and the residual fraction (F4). All the details of the procedure above were published in our previous report (Xiong et al., 2018).

2.6. Conditioning efficiency assessment

2.6.1 Sludge dewaterability

The sludge dewaterability was evaluated by the capillary suction time (CST) which was measured using a 304M CST instrument (Triton, UK). The CST reduction efficiency (Y), which was used to assess the conditioning efficiency of hydrothermal treatment, can be obtained as follows:

$$Y = (CST_b - CST_a)/CST_a \quad (1)$$

Where:

Y - CST reduction efficiency (%),

CST_b - the initial CST of the RS (s), and

CST_a - the CST of the sludge after hydrothermal conditioning (s).

2.6.2 Bioavailability of the P and HMs

The existing forms of the P and HMs in the solid products can indicate their bioavailability. The proportions of H_2O-P and $NaHCO_3$-P represent the bioavailable P. The proportion of the F1 concentration indicated the toxicity and bioavailability of HMs.

2.6.3 Heavy metal risk assessment method

The geo-accumulation index (I_{geo}), monomial potential ecological risk factor (E_r) and potential ecological risk index (RI) were used to assess the potential ecological risks of the HMs in the RS and sludge cakes after the hydrothermal treatment (Yu et al., 2011, Huang et al., 2011), which can be calculated as follows:

$$I_{geo} = \log_2 \frac{C_i}{1.5B_i} \quad (2)$$

where C_i is the sum of the F1 and F2 contents of the HM (mg/kg) and B_i is the HM mean background value in Chinese soil (mg/kg).

$$E_r = T_r C_i / C_r \quad (3)$$

$$RI = \sum E_r \quad (4)$$

where T_r is the toxic response factor of the HMs and C_r is the background value of soil in Wuhan city (Cheng et al., 2014). The values of T_r and C_r are shown in Table S3 (Chen et al., 2020). Table S4 shows the assessment of these three indexes (Huang and Yuan, 2016).

2.7. Analysis

SPSS 19.0 was used for the statistical analyses, and the influence of different hydrothermal conditions on the P and HMs transformation was analyzed by one-way ANOVA (Tukey's test); $p < 0.05$ represented a significant different.

3. Results and discussion

3.1. RSM optimization results

Seventeen experiments with different formulations for RSM were conducted to optimize the temperature, time, and SPS concentration for sludge hydrothermal conditioning, with the CST reduction efficiency as the response value. The second-order polynomial Equation (5) was obtained after the data fitting and regression analysis as follows:

$$Y = 20.60 + 0.39A + 8.36B + 0.43C + 6.0\times10^{-3}AB + 1.45\times10^{-3}AC + 0.035BC - 2.15\times10^{-3}A^2 - 3.10B^2 - 2.49\times10^{-3}C^2 \quad (5)$$

where Y is the CST reduction efficiency (%), A is the hydrothermal conditioning temperature (°C), B is the hydrothermal conditioning time (h), and C is the SPS concentration (mg/g DS). The model for the CST reduction efficiency was significant for an F-value of 58.60 and Prob > F<0.0001 according to the analysis of variance

regression (Table 3). The "lack of fit F-value" was 2.91, indicating that there was a 16.41% chance that the lack of fit occurred due to noise. The "Adeq precision" reached 20.908, which implied that the designed model could predict the sludge dewaterability correctly. The "predicted R^2" of 0.8498 was reasonably consistent with the "Adj R^2" of 0.9701, indicating that the model could reliably describe the effects of hydrothermal temperature, time, and concentration of SPS on the sludge dewatering performance. In addition, the regression factor (R^2) of the model was 0.9869. All the above analyses indicated that the model was significant. The low value of the coefficient of variance (CV) (1.17%) indicated that the experimental results had high repeatability. In this model, A, B, C, AC, BC, A^2, B^2, and C^2 were significant because their values of "Prob > F" were lower than 0.05. The predicted versus actual values for the CST reduction efficiency are shown in Fig. S1, which indicated that the model was adequate and reliable, as the majority of the data points were close to the regression line.

Table 3 Analysis of variance regression model for CST reduction efficiency.

Source	Sum of squares	df	Mean square	F-Value	P-Value (Prob > F)
Model	486.78	9	54.09	58.60	<0.0001
A-Temperature	11.28	1	11.28	12.22	0.0100
B-Time	35.28	1	35.28	38.23	0.0005
C-SPS	14.85	1	14.85	16.09	0.0051
AB	0.36	1	0.36	0.39	0.5521
AC	52.56	1	52.56	56.95	0.0001
BC	12.25	1	12.25	13.27	0.0083
A^2	121.76	1	121.76	131.93	<0.0001

B^2	40.53	1	40.53	43.91	0.0003
C^2	163.29	1	163.29	176.93	<0.0001
Residual	6.46	7	0.92		
Lack of fit	4.43	3	1.48	2.91	0.1641
SD	0.96	R^2		0.9869	
Mean	82.16	Adjusted R^2		0.9701	
CV%	1.17%	Predicted R^2		0.8498	
PRESS	74.09	Adeq Precision		20.908	

Fig. 1 shows the contour and 3D response surface plots of the proposed model for CST reduction efficiency. The interaction of the other two variables was investigated when the third factor was retained at zero levels. Fig. 1(a) displays the interaction between the hydrothermal temperature and time which indicated that the CST reduction efficiency increased as the hydrothermal time was within the range of 1-2 h. The highest CST reduction efficiency was recorded when the hydrothermal time ranged from 1.5 - 2 h and the temperature was 140-150 °C. Gao et al. (2019) investigated the effect of the temperature and time of hydrothermal carbonization on sludge dewatering by coupling with mechanical compression. They reported that the optimal temperature was 160-240 °C. In addition, an increase in the time had a negligible or slight effect on the CST reduction efficiency. Fig. 1(b) indicates that at a higher temperature (180-200 °C), the CST reduction efficiency could hardly be affected by the increase in SPS concentration. The CST reduction efficiency demonstrated a U-curve with an increasing SPS concentration when the temperature was in the range of 120-160 °C. Fig. 1(c) shows the interactive influence between the hydrothermal time and SPS concentration. At longer durations (2-3 h), the CST reduction efficiency changed slightly with an increase

in time. The CST reduction efficiency showed a U-curve with an increasing SPS concentration. Park et al. (2018) found that the properties of the hydrochar and biomass dewaterability could improve with a hydrothermal treatment time of 1 h. We found that the significant influencing factors on the CST reduction efficiency in the experiment were the hydrothermal temperature and SPS concentration. Han et al. (2019) found that the temperature of the thermal hydrolysis pretreatment had a larger effect on the P complexation of sewage sludge than the reaction time. The optimal experimental conditions obtained from the RSM model of the hydrothermal temperature, time, and SPS concentration were found to be 145 °C, 2 h, and 150 mg/g, respectively. The optimal dewatering conditions were confirmed by five comparison experiments.

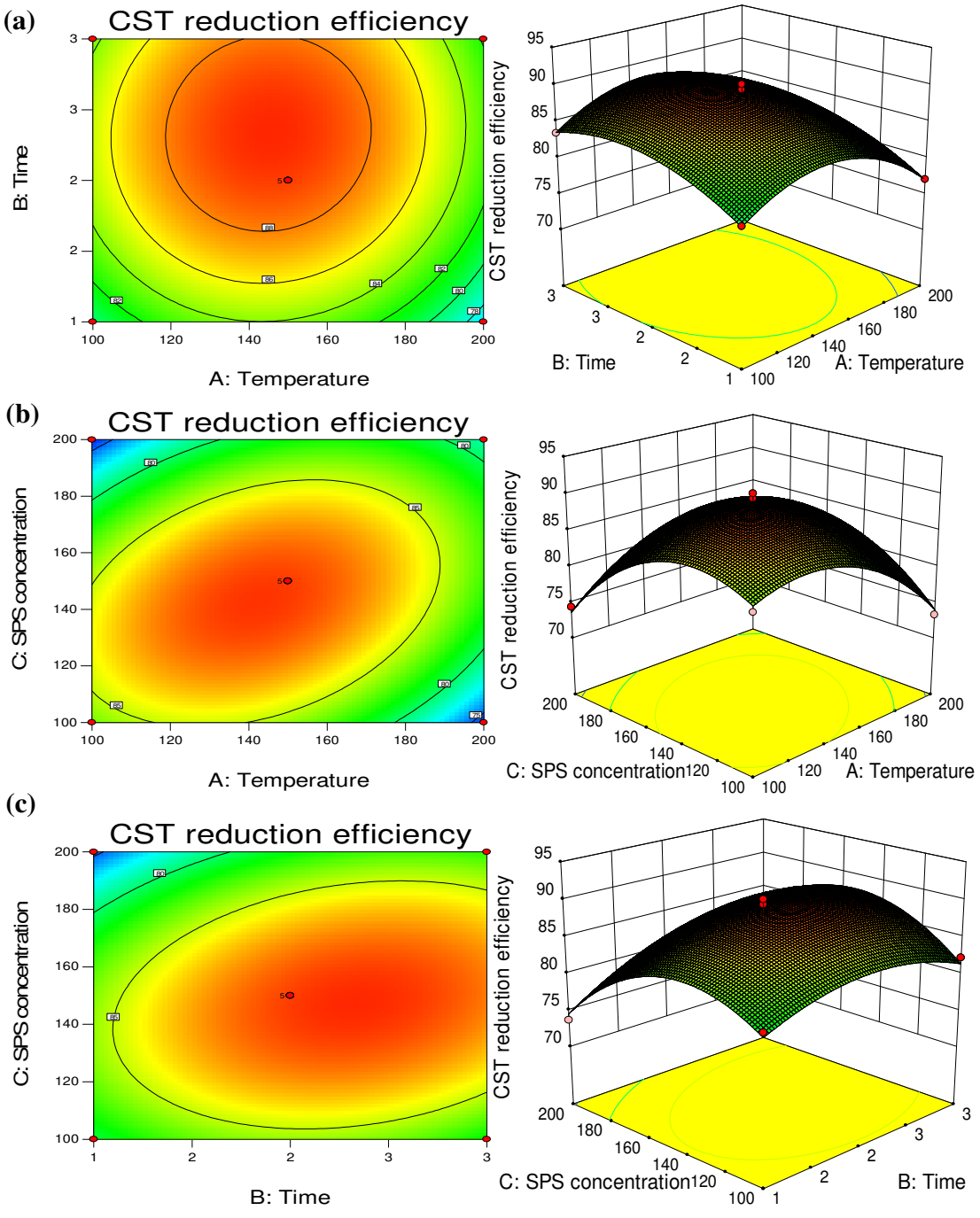

Fig. 1. Contour and 3D response surface plots: (a) hydrothermal time and temperature; (b) temperature and SPS concentration, and (c) time and SPS concentration.

3.2. P transformation during hydrothermal conditioning with different SPS concentrations

3.2.1 Effects of the SPS concentration on the distribution of P between the liquid and solid

The distribution of the P between the liquid and sludge cake is shown in Table S3. The results demonstrated that large proportions of the initial P were retained in the sludge cakes, which was consistent with other reports (Dai et al., 2015). The results of their study suggested that hydrothermal carbonization could efficiently immobilize P in cow manure. The unit mass of P in sludge cakes clearly increased after the hydrothermal treatment owing to the volatilization of organic matter (Han et al., 2019). In addition, the hydrothermal treatment process may suppress the P release into liquid; therefore, P was retained on the hydrochar of sewage sludge. P gradually increased in the sludge cakes with an increasing SPS concentration due to the degradation of organic sludge flocs being promoted by $SO_4^{\bullet -}$ radicals (Zhen, et al., 2012). P was released from the sludge cells during the hydrothermal process and, combined with Fe, Al, Mg, and Ca (Appels et al., 2008). Thus, the addition of SPS could inhabit the release of P into the liquid and promote P enrichment in the sludge cakes.

3.2.2 Operational speciation of P

Fig. 2 shows that P in sequential extracts of the RS and sludge cakes after the hydrothermal treatment with different SPS concentrations showed different fractionation behaviors. Generally, the H_2O-P and $NaHCO_3$-P contents in the sludge cakes after the hydrothermal treatment were lower than those in RS. This result indicated that the hydrothermal treatment decreased the P bioavailability of the sludge cakes, and the same finding was reported by (Huang et al., 2017). After the

hydrothermal treatment, H_2O-P and $NaHCO_3$-P decreased with increasing HCl-P and Residue-P contents. The decrease in the P bioavailability may be because orthophosphates degraded from organophosphates formed phosphate precipitates (e.g., calcium phosphate) or adsorbed to minerals in the sludge; therefore unstable inorganic P may also be transferred to more stable P species due to dissolution or recrystallization (Huang and Tang, 2016). The amounts of H_2O-P and $NaHCO_3$-P decreased to 0.015 mg/g DS and 0.38 mg/g DS, respectively, after the hydrothermal treatment with 200 mg/g DS SPS compared to 0.917 mg/g DS and 2.81 mg/g DS for RS. These results indicated that the addition of SPS promoted P release from the sludge cells through oxidation by the $SO_4^{\bullet -}$ radicals, and the released P transformed into more stable P species. For instance, amorphous Ca-Mg P could crystallize to form less soluble phosphates, such as apatite (Xu et al., 2018).

In addition, the content of H_2O-P is commonly used to assess the liability of P loss from solid P fertilizer for land utilization because the discharge of P can result in the eutrophication of aquatic ecosystems (Liu et al., 2019). Based on the above analysis, it can be concluded that the addition of SPS during the hydrothermal conditioning process could fix P in sludge and inhibit the eutrophication.

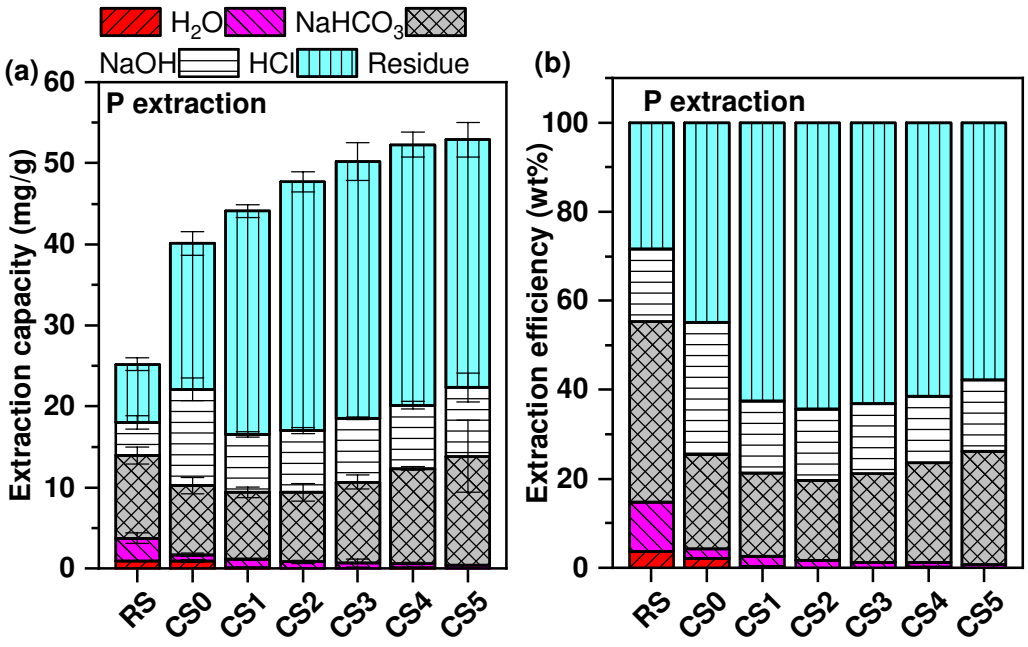

Fig. 2. Distribution of P in sequential extracts of the RS and sludge cakes after hydrothermal treatment with different SPS concentrations. The extraction efficiency (wt%) was obtained by the ratio of extracted Total P to Total P in the sample. Each data point was the average of results from three independent extraction experiments.

3.3. Transformation of HMs during hydrothermal conditioning with different SPS concentrations

3.3.1 Total HMs contents in the liquid and solid

The total contents of Cu, Zn, Ni, Pb and Cr in the RS, liquid and sludge cakes after the hydrothermal treatment are shown in Table 4. The above HMs were studied for their relatively high content in the RS. The results suggested that more than 90% of all HMs were retained in the sludge cakes, which was consistent with other reports (Leng et al., 2014; Liu et al., 2018). According to HMs contents, RS contained higher contents of Cu and Zn, less Pb and Cr, and the lowest concentration of Ni, which was in accordance with the results reported by Shi (2013).

After the hydrothermal treatment, the variation in HMs in the sludge cakes was similar to that of the HMs in RS. Compared with HMs content in RS, there was an increased in the sludge cakes, which was mainly attributed to the degradation of organic matter in the sludge during hydrothermal treatment (Chen, et al., 2017).

304 **Table 4** Heavy metal content of the raw sludge, liquid and sludge cakes after the hydrothermal treatment (mg/kg)

	RS	S0		S1		S2		S3		S4		S5	
HM		Liquid	Cake	Liquid	Cake	Liquid	Cake	Liquid	Cake	Liquid	Cake	Liquid	Cake
Cu	344±63.2	0	377±14.5	0	336±32.5	0	341.5±31.8	0	368±31.1	0	530.5±17.7	0	406±28.3
Ni	29.6±2.7	2.28±1.13	68.8±12.2	4.35±0.07	67.5±10.6	3.8±0.28	62±7.07	4.15±0.07	67.5±6.4	4.3±0.28	99.5±2.1	4.05±0.49	81±5.6
Pb	206.4±45.2	0	140.5±41.9	6.55±1.06	94.5±71.4	5.85±0.07	113±26.9	5.65±1.49	161.5±50.2	6.25±0.12	224.5±0.71	6.7±1.13	151±13.4
Zn	1301±112.3	0.33±0.23	1707±94.2	0	1369±53.7	0	1362±49.5	0	1457±54.4	0	1905±86.3	0	1599±54.4
Cr	167±22	6.43±2.13	303.8±21.1	12.05±0.07	289±11.3	11.1±0.07	293±9.90	11.1±0.28	300.5±10.6	12.05±0.07	428±12.7	11.7±0.71	315±11.3

305

306 3.3.2 Fraction distribution of HMs in the sludge cakes

307 The distribution of four fractions (F1-soulable and exchangeable, F2-reducible,
308 F3-oxidizable, F4-residue) of Cu, Ni, Pb, Zn and Cr in the RS and sludge cakes are
309 shown in Fig. 3; these results, were obtained by the BCR sequential extraction scheme.
310 The mass percentage of the oxidizable and residual fractions of Cu accounted for 69%
311 in the RS. Hu et al. (2018) also reported that Cu always existed as oxidizable and
312 residual fractions that had high bioavailability and mobility. The percentage in the
313 oxidizable fraction clearly increased after the hydrothermal treatment (48.4% for CS0,
314 75.1% for CS1, 72.2% for CS2, 69.6% for CS3, 48.7% for CS4, 59.4% for CS5),
315 indicating that Cu was mainly bound to the organic matter and sulfides in the RS and
316 sludge cakes after the hydrothermal treatment. The exchangeable and reducible fraction
317 of Cu decreased, suggesting less mobility and potential bioavailability of Cu after the
318 hydrothermal treatment (Kazi et al., 2005).

319 The variation trend of Ni was similar to that of Cu except for the sludge cake
320 obtained without the addition of SPS. In the RS, the mass percentage of the oxidizable
321 and residual fractions accounted for as much as 73%. Regarding CS0, the majority of
322 Ni was present in the oxidizable fraction (83%), indicating that it was mainly associated
323 with strong organic ligands. With an increasing of SPS concentration, the residual
324 fraction of Ni increased from 0.65% (CS0) to 62% (CS5) which showed that the toxicity
325 of Ni decreased significantly after the hydrothermal treatment with SPS. The key reason
326 for the above results could be the strong physic-chemical effects and crystalline
327 compound immobilization during the hydrothermal process (Sun et al., 2018).

With respect to Pb in the RS, the highest mass percentage (49.7%) was found in the reducible fraction, suggesting that Pb mainly bound to the Fe and Mn oxides. The exchangeable fraction in the RS was 19.8% and decreased to 1-2% after hydrothermal treatment. Moveover, the residual fraction increased from 22% in the RS to 40-74% in the sludge cakes after the hydrothermal treatment. These results illustrated that the mobility and toxicity of Pb decreased after the hydrothermal treatment, which was in accordance with the results reported by Yuan et al. (2011) and Shao et al. (2015).

Regarding Zn, the mass percentage of the exchangeable and reducible fractions accounted for 65% in the RS, indicating its higher toxicity and availability. He et al. (2010) also found that Zn in sludge mainly presented as a reducible fraction (43.4%), which bound to the Fe and Mn oxides. After the hydrothermal treatment, Zn was mainly present in the oxidizable fraction (40-70%) in all sludge cakes. Chen et al. (2015) also found that Zn easily transferred to the oxidizable fraction during thermal treatment. As the SPS concentration increased, the residual fraction of Zn increased from 15% in CS1 to 32% in CS5. The exchangeable fraction of Zn decreased from 32.8% in RS to 3.7% in CS5, showing the immobilization of Zn after the hydrothermal treatment with SPS.

Unlike Cu, Ni, Pb and Zn, the highest percentage of Cr was found in the residual fraction (85%) in the RS, decreasing to 5.8% in the CS0 after hydrothermal treatment, and increasing to 80% with the addition of SPS. Shao et al. (2015) also reported that Cr in municipal sewage sludge mainly existed as residual fraction. Cr was prone to transfer to unstable fractions during the hydrothermal treatment. SPS could promote the oxidation of these insoluble Cr fractions to stable Cr complexes. The exchangeable

fraction increased from 1% in RS to 2.7% in CS0 and then decreased to 0.5% in CS5. These results showed that the addition of SPS was good for the immobilization of Cr. It was also reported in our previous work that the addition of SPS could reduce the risk of HMs during the conditioning of sewage sludge by Fe^{2+}-sodium persulfate oxidation and rice husk (Xiong et al., 2018).

Comparing the residual fractions of Cu, Ni, Pb, Zn and Cr in the RS and all sludge cakes, it can be found that the addition of SPS during the hydrothermal treatment of sludge could immobilize HMs.

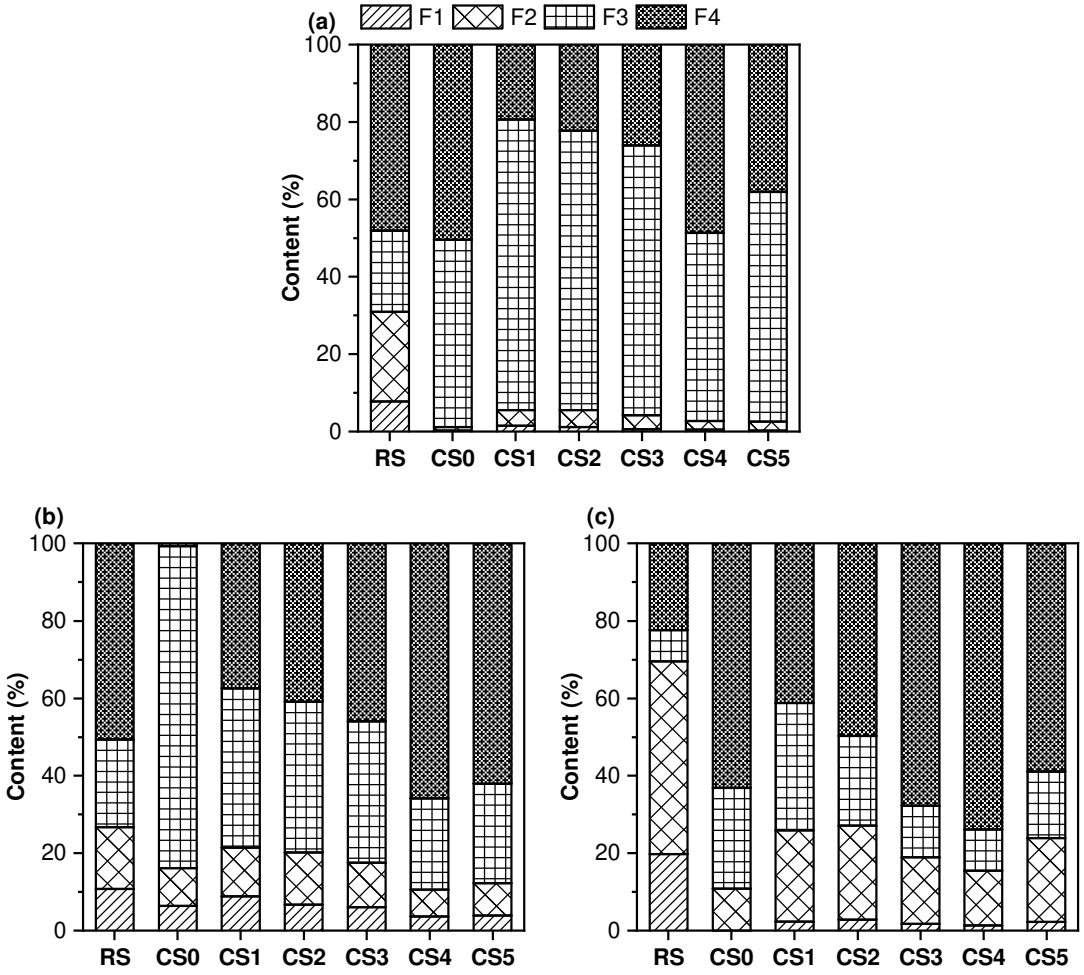

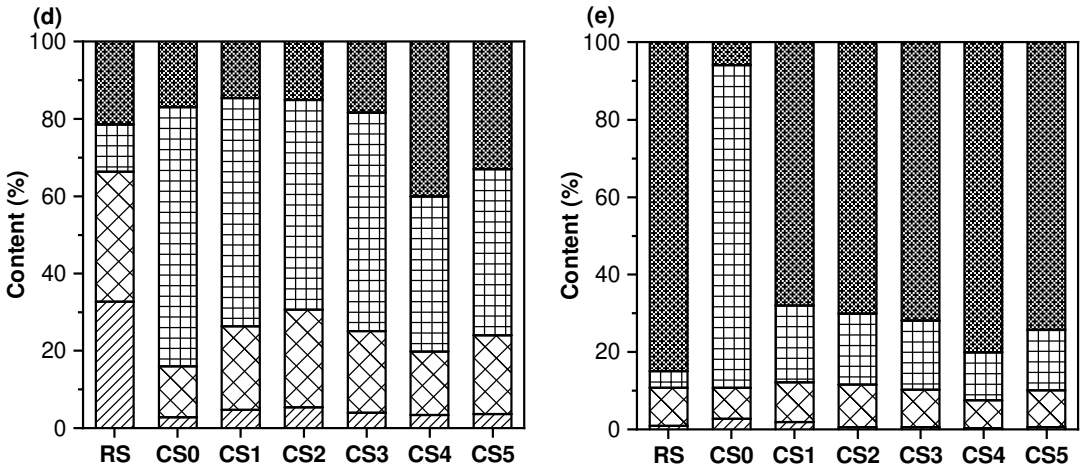

Fig. 3. Distribution percentages of the various fractions of (a) Cu, (b) Ni, (c) Pb, (d) Zn and (e) Cr in the sludge cakes. F1: exchangeable fraction, F2: reducible fraction, F3: oxidizable fraction, and F4: residual fraction.

3.4. Environmental risk assessment of the HMs

Fig. 4 shows the values of I_{geo}, E_r, and RI. Regarding the RS, the I_{geo} value of Cu and Pb was between 0 and 1, which indicated that Cu and Zn were uncontaminated to moderately contaminated in the environment. The I_{geo} value of Zn was between 1 and 2, which demonstrated that Zn was moderately contaminated. The I_{geo} values of Ni and Cr were below 0, which meant that Ni and Cr demonstrated practically uncontaminated. Except for Zn, the I_{geo} values of Cu, Ni, Pb, and Cr of all the conditioned sludge cakes were below 0, indicating that Cu, Ni, Pb, and Cr demonstrated practically uncontaminated in the environment. E_r represents the toxicity of the different HMs. It was obvious that the E_r value of the conditioned sludge cakes decreased compared with that of the RS. The E_r value of all samples was below 40, indicating that the ecological risk of the RS and sludge cakes was low. The potential ecological risk of the HMs was Pb>Cu>Zn>Ni>Cr based on the E_r value. According to the value of *RI*, the ecological

risk level of the RS and all conditioned sludge cakes was low in the environment. These results indicated that the ecological risk indexes of the HMs decreased after the hydrothermal treatment, which was in agreement with the analysis of the fraction distribution in Section 3.3.2.

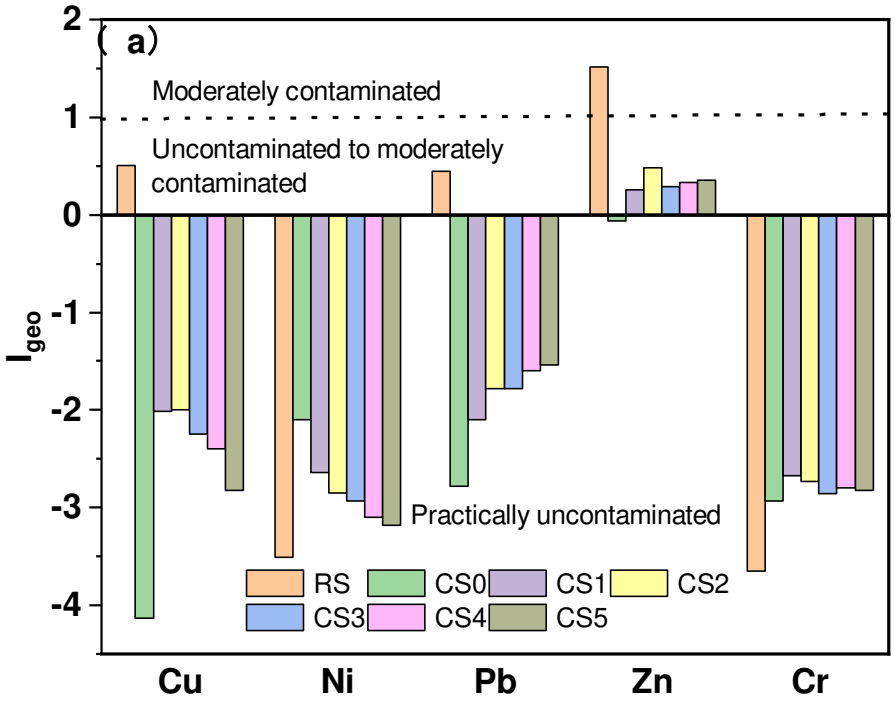

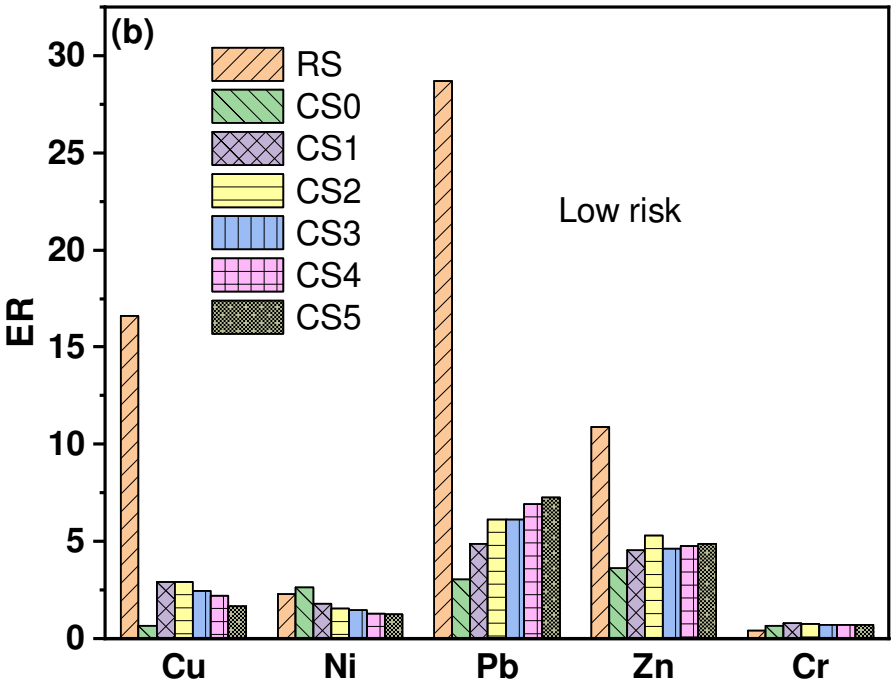

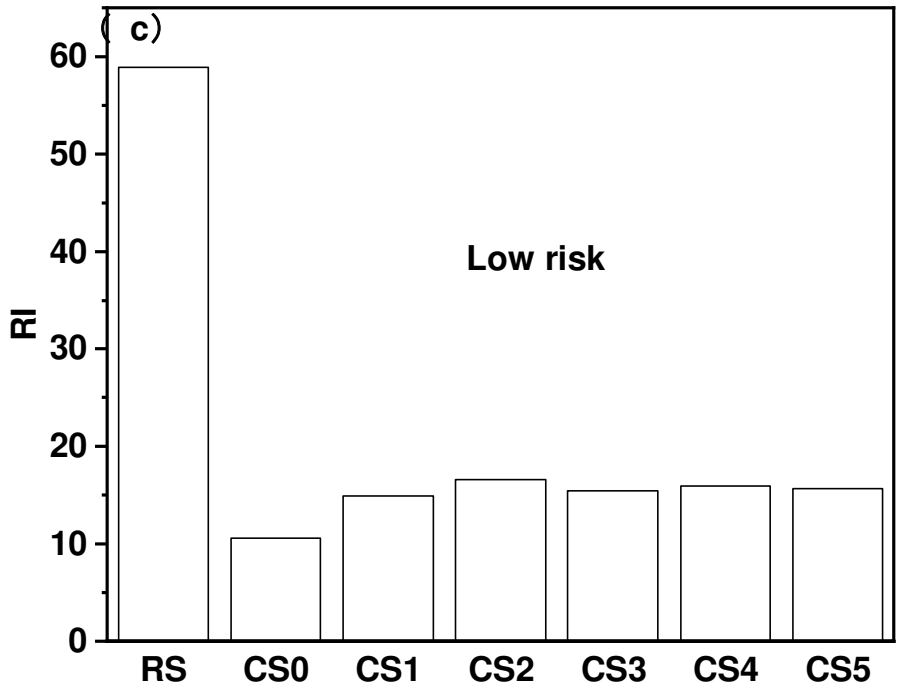

Fig. 4. (a) the geo-accumulation index (I_{geo}), (b) potential ecological risk factor (E_r), and (c) potential ecological risk index (RI) of HMs in RS and conditioned cakes,

4. Conclusions

This study investigated P and heavy metals transformation during the hydrothermal treatment of sewage sludge to improve sludge dewaterability. The optimal hydrothermal temperature, time, and concentration of persulfate were 145 °C, 2 h, and 150 mg/g DS, respectively; these parameters were determined by a three-level and variable Box-Behnken design. Different concentrations of persulfate were added to explore its effects on the P and heavy metals distribution and transformation during hydrothermal treatment with sewage sludge. Only a small proportion of P transferred into the liquid products after the hydrothermal treatment. The extraction capacity and efficiency of P sequential extraction indicated that the hydrothermal treatment decreased the P bioavailability of the sludge cakes. Residue-P in the sludge cakes increased as the persulfate concentration increased. According to the results of the

fraction distribution of HMs in the sludge cakes and the environmental risk assessment of HMs, it can be concluded that the addition of persulfate during the hydrothermal treatment of sludge could immobilize the HMs. These results indicated that the combination of persulfate and hydrothermal technology to treat sludge would have a nonnegligible effect on the sludge dewatering performance and P and heavy metals fractions, which could be considered during sludge reclamation.

Ethics approval and consent to participate

Not applicable

Consent for publication

Not applicable

Availability of data and materials

All data generated or analyzed during this study are included in this published article [and its supplementary information files].

Competing interests

The authors declare that they have no competing interests" in this section.

Funding

This work was supported by the National Natural Science Foundation of China (51908233).

Authors' contributions

Qiao Xiong: Methodology, Software, Formal analysis, Investigation, Writing - original draft. **Jing Xia**: Investigation. **Xiang Wu**: Investigation. **Xu Wu**: Software, Validation. **Haobo Hou**: Supervision. **Hang Lv**: Writing - review & editing.

References

Appels, L., Baeyens, J., Degreve, J., Dewil, R., 2008. Principles and potential of the anaerobic digestion of waste-activated sludge. Prog. Energy Combust. Sci. 34, 755–781.

Chen, H., Zhang, C., Rao, Y., Jing, Y., Luo, G., Zhang, S., 2017. Methane potentials of wastewater generated from hydrothermal liquefaction of rice straw: focusing on the wastewater characteristics and microbial community compositions. Biotechnol. Biofuels 10, 140.

Chen, L.M., Liao, Y.F., Ma, X.Q., Niu, Y.D., 2020. Effect of co-combusted sludge in waste incinerator on heavy metals chemical speciation and environmental risk of horizontal flue ash. Waste Manage. 102, 645-654.

Cheng, X.M., Li, T., Yang, K., Liu, F., Cheng, X.M., 2014. Geochemical background and baseline value of chemical elements in urban coil in China. Earth Science Frontiers, 21, 265-306.

Chen, F.F., Hu, Y.Y., Dou, X.M., Chen, D.Z., Dai, X.H., 2015. Chemical forms of heavy metals in pyrolytic char of heavy metal-implanted sewage sludge and their impacts on leaching behaviors, J. Anal. Appl. Pyrolysis 116, 152–160.

Dai, L., Tan, F., Wu, B., He, M., Wang, W., Tang, X., Hu, Q., Zhang, M., 2015. Immobilization of phosphorus in cow manure during hydrothermal carbonization. J. Environ. Manag. 157, 49-53.

437 Dewil, R, Baeyens, J, Appels, L. 2007. Enhancing the use of waste activated sludge as
438 bio-fuel through selectively reducing its heavy metal content. J Hazard. Mater. 144,
439 703-707.
440 Funke, A., Ziegler, F., 2010. Hydrothermal carbonization of biomass: a summary and
441 discussion of chemical mechanisms for process engineering. Biofuels Bioprod.
442 Bior. 4, 160-177.
443 Gao, N.B., Li, Z.Y., Quan, C., Miskolczi, N., Egedy, A., 2019. A new method combining
444 hydrothermal carbonization and mechanical compression in-situ for sewage
445 sludge dewatering: Bench-scale verification. J. Anal. Appl. Pyrol. 139, 187-195.
446 Hedley, M.J., Stewart, J.W.B., Chauhan, B.S., 1982. Soil Sci. Soc. Am. J. 46, 970.
447 Huang H.J., Yuan, X.Z., 2016. The migration and transformation behaviors of heavy
448 metals during the hydrothermal treatment of sewage sludge. 2016. Bioresour.
449 Technol. 200, 991-998.
450 Hu, Y.Y., Yang, F., Chen, F.F., Feng, Y.H., Chen, D.Z., Dai, X.H., 2018. Pyrolysis of the
451 mixture of MSWI fly ash and sewage sludge for co-disposal: Effect of
452 ferrous/ferric sulfate additives. Waste Manage. 75, 340-351.
453 Han, X.M., Wang, F., Zhou, B.H., Chen, H.L., Yuan, R.F., Liu, S.H., Zhou, X.Q., Gao,
454 L., Lu, Y., Zhang, R., 2019. Phosphorous complexation of sewage sludge during
455 thermal hydrolysis with different reaction temperature and reaction time by K-
456 edge XANES and ^{31}P NMR. Sci. Total Environ. 688, 1-9.
457 Huang, H., Yuan, X., Zeng, G., Zhu, H., Li, H., Liu, Z., Jiang, H., Leng, L., Bi, W., 2011.
458 Quantitative evaluation of heavy metals' pollution hazards in liquefaction residues

459 of sewage sludge. Bioresour. Technol. 102, 10346–10351.
460 Huang, H.J., Yuan, X.Z., 2016. The migration and transformation behaviors of heavy
461 metals during the hydrothermaltreatment of sewage sludge. Bioresour. Technol.
462 200, 991–998.
463 Huang, R.X., Fang, C., Lu, X.W., Jiang, R.F., Tang, Y.Z., 2017. Transformation of
464 phosphorus during (hydro)thermal treatments of solid biowastes: Reaction
465 mechanisms and implications for P reclamation and recycling. Environ. Sci.
466 Technol. 51, 10284-10298.
467 Huang, R.; Tang, Y. 2016. Evolution of phosphorus complexation and mineralogy
468 during (hydro)thermal treatments of activated and anaerobically digested sludge:
469 Insights from sequential extraction and P K-edge XANES. Water Res. 100, 439-
470 447.
471 He, Y.D., Zhai, Y.B., Li, C.T., Yang, F., Chen, L., Fan, X.P., Peng, W.F., Fu, Z.M., 2010.
472 The fate of Cu, Zn, Pb and Cd during the pyrolysis of sewage sludge at different
473 temperatures. Environ. Technol. 31, 567-574.
474 Kazi, T.G., Jamali, M.K., Kazi, G.H., Arain, M.B., Afridi, H.I., Siddiqui, A., 2005.
475 Evaluating the mobility of toxic metals in untreated industrial wastewater sludge
476 using a BCR sequential extraction procedure and a leaching test. Anal. Bioanal. J.
477 Chem. 383, 297-304.
478 Kordkandi, S. A.; Forouzesh, M. 2014. Application of full factorial design for
479 methylene blue dye removal using heat-activated persulfate oxidation. J. Taiwan
480 Inst. Chem. Eng. 45, 2597-2604.

Kepp, U., Machenbach, I., Weisz, N., Solheim, O.E., 2000. Enhanced stabilisation of sewage sludge through thermal hydrolysis – three years of experience with full scale plant. Water Sci. Technol. 42, 89-96.

Liu Q., Fang, Z., Liu Y., Liu Y.Y., Xu Y.F., Ruan X.X., Zhang X.L., Cao W.M., 2019. Phosphorus speciation and bioavailability of sewage sludge derived biochar amended with CaO. Waste Manage. 87: 71-79.

Leng, L., Yuan, X., Huang, H., Chen, X., Zeng, G., 2014. The migration and transformation behavior of heavy metals during the liquefaction process of sewage sludge. Bioresour. Technol. 167, 144-150.

Liu, T.T., Liu Z.G., Zheng Q.F., Lang, Q.Q., Xia, Y., Peng, N.N., Gai, C., 2018. Effect of hydrothermal carbonization on migration and environmental risk of heavy metals in sewage sludge during pyrolysis. Bioresour. Technol. 247, 282-290.

Li, H., Wang, Y., Zheng, H., 2018. Variations of moisture and organics in activated sludge during $Fe^0/S_2O_8^{2-}$ conditioning-horizontal electro-dewatering process. Water Res. 129, 83-93.

Mahmoud, A., Hoadley, A.F.A., Citeau, M., Sorbet, J.M., Olivier, G., Vaxelaire, J., Olivier, J., 2018. A comparative study of electro-dewatering processing performance for activated and digested wastewater sludge. Water Res. 129, 66-82.

Neyens, E., Baeyens, J., Dewil, R., De heyder, B., 2004. Advanced sludge treatment affects extracellular polymeric substances to improve activated sludge dewatering. J. Hazard. Mater. 106, 83-92.

Olivier, J., Conrardy, J.-B., Mahmoud, A., Vaxelaire, J., 2015. Electro-dewatering of wastewater sludge: an investigation of the relationship between filtrate flow rate and electric current. Water Res. 82, 66-77.

Park, K.Y., Lee, K., Kim, D., 2018. Characterized hydrochar of algal biomass for producing for solid fuel through hydrothermal carbonization. Bioresour. Technol. 258, 119-124.

Rauret, G., López-Sánchez, J.F., Sahuquillo, A., Rubio, R., Davidson, C., Ure, A., Quevauviller, P., 1999. Improvement of the BCR three step sequential extraction procedure prior to the certification of new sediment and soil reference materials. J. Environ. Monit. 1, 57-61.

Shi, W.S., Liu, C.G., Shu, Y.J., Feng, C.P., Lei, Z.F., Zhang, Z.Y., 2013. Synergistic effect of rice husk addition on hydrothermal treatment of sewage sludge: fate and environmental risk of heavy metals. Bioresour. Technol. 149, 496-502.

Świerczek, L., Cieślik, B.M., Konieczka, P., 2018. The potential of raw sewage sludge in construction industry: a review. J. Clean. Prod. 200, 342-356.

Saveyn, H., Pauwels, G., Timmerman, R., Van der Meeren, P., 2005. Effect of poly-electrolyte conditioning on the enhanced dewatering of activated sludge by application of an electric field during the expression phase. Water Res. 39, 3012-3020.

Sun, S.C., Huang, X.F., Lin, J.H., Ma, R., Fang, L., Zhang, P.X., Qu, J.L., Zhang, X.H., Liu, Y.L., 2018. Study on the effects of catalysts on the immobilization efficiency and mechanism of heavy metals during the microwave pyrolysis of sludge. Waste

524 Manage. 77, 131-139.
525 Shao, J.G., Yuan, X.Z., Leng, L.J., Huang, H.J., Jiang, L.B., Wang, H., Chen, X.H.,
526 Zeng, G. M., 2015. The comparison of the migration and transformation behavior
527 of heavy metals during pyrolysis and liquefaction of municipal sewage sludge,
528 paper mill sludge, and slaughterhouse sludge. Bioresour. Technol. 198, 16-22.
529 Xiong, Q., Zhou, M., Liu, M.J., Jiang, S.J., Hou, H.B., 2018. The transformation
530 behaviors of heavy metals and dewaterability of sewage sludge during the dual
531 conditioning with Fe^{2+}-sodium persulfate oxidation and rice husk. Chemosphere
532 208, 93-100.
533 Xu, Y. F., Yang, F., Zhang, L., Wang X., Sun, Y., Liu, Q., Qian G.R., 2018. Migration
534 and transformation of phosphorus in municipal sludge by the hydrothermal
535 treatment and its directional adjustment. Waste Manage. 81, 196-201.
536 Xu, Q., Wang, Q., Zhang, W., Yang, P., Du, Y., Wang, D., 2018. Highly effective
537 enhancement of waste activated sludge dewaterability by altering proteins
538 properties using methanol solution coupled with inorganic coagulants. Water Res.
539 138, 181-191.
540 Yu, G.B., Liu, Y., Yu, S., Wu, S.C., Leung, A.O., Luo, X.S., Xu, B., Li, H.B., Wong,
541 M.H., 2011. Inconsistency and comprehensiveness of risk assessments for heavy
542 metals in urban surface sediments. Chemosphere 85, 1080-1087.
543 Yu, Y., Yang, X., Lei, Z.F., Yu, R., Shimizu, K., Chen, N., Feng, C.P., Zhang, Z.Y., 2019.
544 Effects of three macroelement cations on P mobility and speciation in sewage
545 sludge derived hydrochar by using hydrothermal treatment. Bioresour. Technol.

546 Reports 7, 100231.
547 Yuan, X.Z., Huang, H.J., Zeng, G.M., Li, H., Wang, J.Y., Zhou, C.F., Zhu, H.N., Pei,
548 X.K., Liu, Z.F., Liu, Z.T., 2011. Total concentrations and chemical speciation of
549 heavy metals in liquefaction residues of sewage sludge. Bioresour. Technol. 102,
550 4104-4110.
551 Zhen, G., Lu, X., Zhao, Y., Chai, X., Niu, D., 2012. Enhanced dewaterability of sewage
552 sludge in the presence of Fe(II)-activated persulfate oxidation. Bioresour. Technol.
553 116, 259-165.
554 Zhang, X.Z., Huang, Y.Q., Song, Y.P., Zhan, H., Yin, X.L., Wu, C.Z. 2017. The
555 transformation pathways of nitrogen in sewage sludge during hydrothermal
556 treatment. Bioresour. Technol. 245, 463-470.
557 Zhen, G.; Lu, X.; Zhao, Y.; Chai, X.; Niu, D. 2012. Enhanced dewaterability of sewage
558 sludge in the presence of Fe(II)-activated persulfate oxidation. Bioresour. Technol.
559 116, 259-265.
560 Zhang, G.M., Yang, J., Liu, H.Z., Zhang, J., 2009. Sludge ozonation: Disintegration,
561 supernatant changes and mechanisms. Bioresource Technol. 100, 1505-1509.

Supplementary Files

This is a list of supplementary files associated with this preprint. Click to download.

- Supplementarymaterial413.docx